

# A Novel Multiresolution based Optimization Scheme for Robust Affine Parameter Estimation

J.Dinesh Peter

**Abstract**—This paper describes a new method for affine parameter estimation between image sequences. Usually, the parameter estimation techniques can be done by least squares in a quadratic way. However, this technique can be sensitive to the presence of outliers. Therefore, parameter estimation techniques for various image processing applications are robust enough to withstand the influence of outliers. Progressively, some robust estimation functions demanding non-quadratic and perhaps non-convex potentials adopted from statistics literature have been used for solving these. Addressing the optimization of the error function in a factual framework for finding a global optimal solution, the minimization can begin with the convex estimator at the coarser level and gradually introduce non-convexity i.e., from soft to hard redescending non-convex estimators when the iteration reaches finer level of multiresolution pyramid. Comparison has been made to find the performance of the results of proposed method with the results found individually using two different estimators.

**Keywords**—Image Processing, Affine parameter estimation, Outliers, Robust Statistics, Robust M-estimators

## I. INTRODUCTION

Estimation techniques are basic chore in many in computer vision applications. The ultimate aim of the estimation techniques is to estimate geometric, photometric and semantic information as accurate as possible. Robust affine parameter estimation technique has been used here in order to reduce the impact of outliers towards the estimation of parameters. In general, the robust estimators do not provide closed form solutions, and often result in an objective function that is non-convex. Still some stochastic minimizations such as stochastic relaxation, simulated annealing [1-3] and finite search methods [4-7] can be explored to find the global minimum, but they have limited capability for avoiding local minima. Their performance depends on the initialization quality and computationally complexity [8]. So we need to find a factual framework for the minimization scheme that is more efficient, practical and computationally fast. Some of the factual frameworks in the literatures are in [9-11]. Researchers of paper [12] derived a convergence sufficient condition using fourier decomposition for the minimization of the energy function. But this can be applied for particular case of a transformation space reduced to global translations. This paper proposed a novel factual framework minimization with the help of multiresolution strategy and robust statistics that can be applicable for all the case of transformation cases. Three robust M-estimators are suggested in the order from their property of convexity to non-convexity in Table 1.<sup>1</sup>Following the idea as

in the Graduated Non-Convexity (GNC) algorithm described in [13], Non-convexity is gradually acquainted from convexity by using the chosen robust M-estimators when multiresolution pyramid scheme reaches its finer resolution. This method is named as *Acquainted non-convexity multiresolution based optimization scheme (ANMO)*. This results in a new and non-monitored robust affine parameter estimation.

The rest of the paper is organized as follows. Section 2, explains the methodology followed for the affine parameter estimation using the proposed approach. Section 3 compares the estimation accuracies of the proposed scheme with various parameter estimation techniques. Section 4 concludes the paper.

## II. METHODOLOGY

This paper first gives a description of some robust estimation methods used to estimate the affine parameters. Second, explains how the multiresolution pyramid strategy can be utilized to estimate the precise affine parameters using various robust estimation functions applied continuously at each level. The estimated affine parameters are applied to the source image of next level of resolution, and new affine parameters are estimated between the newly warped source image and target image.

### A. Estimation function selection

Estimation function is the function of intensities. The properties that should be satisfied for the estimation functions in parameter estimation problem have been defined in various works in the literature. Researchers of papers [14-17] have preferred using convex potentials in order to ensure the uniqueness of the solution. But the non-convex potentials may be suitable for the images containing high range of outliers. However this option results to some mathematical difficulties and unstableness associated to the existence of local minima. Though the convex potentials give closed form solutions, the influence of outliers is therefore not null. This paper describes the use of three different robust M-estimators in the parameter estimation problem. Among these, one is convex potential and the other two are non-convex potentials (see Table 1).

The chosen convex potential is *Charbonnier* objective function  $E_{CH}$  [18]. The corresponding influence function is monotonic and bounded. It has an advantage that its weight function exists in all  $x$  and is always strictly positive. Since  $E_{CH}$  is continuous, strictly increasing and differentiability is desirable

<sup>1</sup>For  $128 \times 128$  input images, there will be three levels of resolution in multiresolution pyramid scheme.

TABLE I  
 ROBUST OBJECTIVE FUNCTIONS AND ITS PROPERTIES

Property	Robust function	Objective function $\mathfrak{R}(x)$	Influence function $\psi(x)$
Convex	Charbonnier $E_{CH}$	$2\sqrt{1 + (\frac{x}{\sigma})^2} - 2$	Monotone
Nonconvex	Hebert-Leahy $E_{HL}$	$\log(1 + (\frac{x}{\sigma})^2)$	Soft Redescender
Nonconvex	Tukey's Biweight $E_T$	$\left( \begin{array}{l} \frac{x^2}{\sigma^2} - \frac{x^4}{\sigma^4} + \frac{x^6}{3\sigma^6} \\ \frac{1}{3} \end{array} \right) \begin{array}{l}  x  \leq \sigma \\ otherwise \end{array}$	Hard Redescender

for  $\psi$ , the solution to the minimization problem always exists, avoids mathematical instability and it is unique [19]. Since the resulting function to be minimized is convex, there is a guarantee of minimization up to global minimum. Though it forms a closed form solution, the influence function describes that outliers will be handled in a little way. Charbonnier function  $E_{CH}$  also satisfies the following conditions suggested by [18].

- \*  $E_{CH}$  is continuous and strictly decreasing on  $[0 + \infty]$  (See Fig.1(a)).
- \*  $\lim_{(\frac{x}{\sigma}) \rightarrow +\infty} E_{CH} = 0$  (For larger distance (Outliers), Weights are Zero).
- \*  $\lim_{(\frac{x}{\sigma}) \rightarrow 0+} E_{CH} = W, 0 < W < +\infty$  (From smaller to medium values, considerable weights are provided.)

The other chosen non-convex potentials are Hebert-Leahy  $E_{HL}$  [20] and Tukey's biweight  $E_T$  functions. To ensure the goal of robustness, a redescending norm (Influence function or  $\psi$ -function) is required. From this point of view, hard redescending norm such as  $E_T$  is more attractive to outliers. Fig.1(a) shows the influence functions ( $\psi$ -functions) of the various robust objective functions given in Table.1.

While analyzing the weighting functions of the chosen robust functions given in Fig.1(b), one can understand that a hard redescending norm such as Tukey's biweight function  $E_T$  has the horizontal asymptote behavior as the residuals goes to infinity where the other two functions do not have. Hard redescending norms yield highly non-convex potentials, which lead the minimization steps up to local minimum only. So an efficient factual framework can however be determined in this instance for reducing the influence of outliers as well as the minimization up to global minimum. This can be achieved by employing gradual acquaint of non-convexity from convexity in the multiresolution based minimization scheme. The method proposed in next section will explain the same idea for estimating exact affine parameters.

### B. Acquainted Non-convexity Multiresolution based Optimization (ANMO)

A coarse to fine strategy is followed in this case. The chosen convex estimator is used at the coarser resolution. Since the convex estimators are much sensible to the outliers, non-convex M-estimators are acquainted from the next resolution onwards. The main problem of using non-convex estimator is; the solution is attempted only through several locally minimum values, so no uniqueness of the solution is found. Since the previous estimates have placed us within a "basin of attraction"

of the global minimum [21] and also the iterative and incremental sections of the multiresolution pyramid approach make the non-convex estimation to find almost optimally minimum values, thanks to multiresolution scheme. Depends upon the normal distribution of the weighting functions in the pyramid generation, one can choose non-convex M-estimators from their property of soft redescending norm to hard redescending norm. At the middle levels of Gaussian pyramid scheme, the impact of outliers are started to visible. So choosing soft redescending norm at this stage improves the parameter estimation by finding optimally minimum values. And at the finer resolution, the impact of outliers is more, so hard redescending norm is required to reduce the influence of outliers dramatically. The parameters estimated at the finer resolution will be used to warp (or project) the original source.

The number of levels of the multiresolution scheme varies depending on the size of the image. For  $64 \times 64$  and  $128 \times 128$  images, gaussian pyramidal scheme creates two and three levels of resolution respectively. Depending upon the number of levels of resolution in multiresolution pyramid approach, different robust norms can be selected for operation. Fig.2 shows the overview of the proposed scheme for optimization to estimate accurate affine parameters. This methodology obviously reduces the complexity of Graduated Non-convexity algorithm proposed by Black and Zisserman [13] and its application to parameter estimation in [22]. The advantage of using multiresolution refinement strategy is that it does not get trapped into a false local minimum. The results show the power of affine parameter estimation.

### C. Robust Affine parameter estimation

Two images from image sequences for affine parameter estimation are represented as  $I_{x,y,t}$  and  $I_{x,y,t-1}$ .<sup>2</sup> In this paper, the idea of parameter estimation is based on gradient constraints (spatial/temporal derivatives) and the basic flow of the algorithm follows the principles carried on [22]. The error function chosen here is sum of squared difference (SSD). This error function is easy to compute and the minimization will also be simple and it yields good results for the images having identical intensity transformation. For the spatial neighborhood  $\Xi$  of two images, the error function can be written as:

$$E_n(\vec{P}) = \sum_{x,y \in \Xi} \left[ I_{x,y,t} - I_{P_1 x + P_2 y + P_3, P_3 x + P_4 y + P_6, t-1} \right]^2 \quad (1)$$

where  $\vec{P} = (\vec{P}_1, \dots, \vec{P}_6)^T$  represents the affine parameters. In order to give attention to the outliers in an image, a robust

<sup>2</sup>These unconventional notations are representing any two images from an image sequence with the temporal parameter  $t$ . These notations have been used only for mathematical consistency.

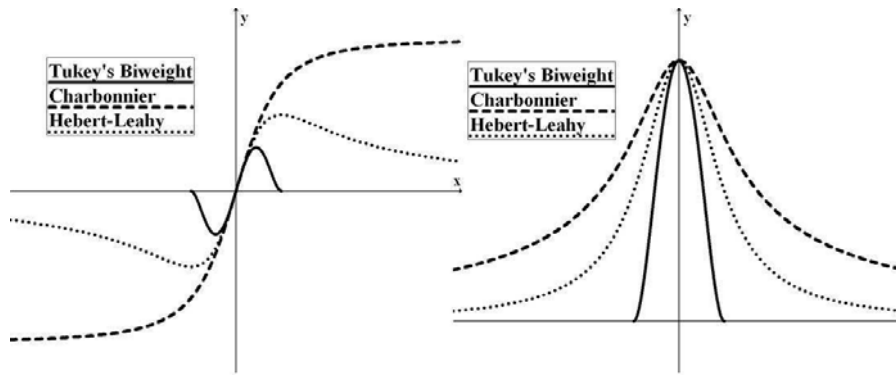


Fig. 1. (a)Influence functions ( $\psi$ -functions), (b)weight functions of the chosen M-Estimators shown in Table.1

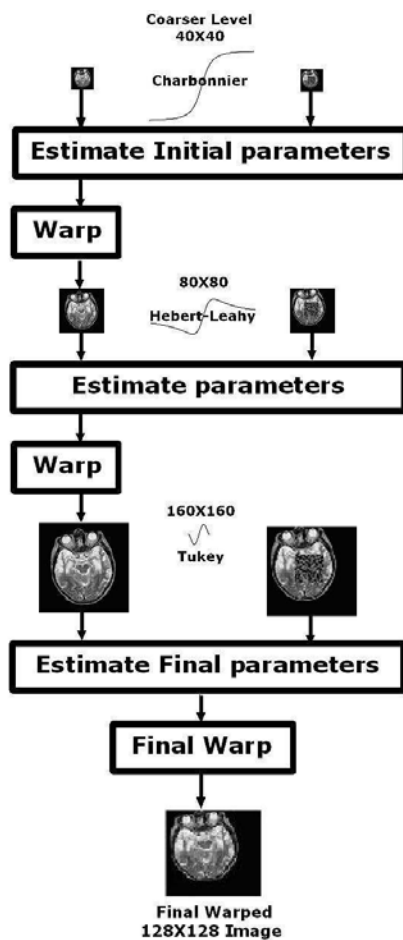


Fig. 2. Overview of Affine parameter estimation using acquainted non-convexity multiresolution based optimization for  $128 \times 128$  images

objective function is applied in the error function in (2). Since the error function is nonlinear in its unknown affine parameters, it cannot be minimized analytically. In order to simplify the minimization, first order truncated Taylor series approximation is involved here.

$$E_n(\vec{P}) \approx \sum_{x,y \in \Xi} \Re \left\{ \left[ I_{x,y,t} - \left( I_{x,y,t} + (P_1x + P_2y + P_5 - x)I_{x,y,t}^x + \right. \right. \right.$$

$$\left. \left. + (P_3x + P_4y + P_6 - y)I_{x,y,t}^y - I_{x,y,t}^t \right) \right]^2, \sigma \} \quad (2)$$

where  $I_{x,y,t}^x$  and  $I_{x,y,t}^y$  are spatial derivatives and  $I_{x,y,t}^t$  is temporal derivative. The robust error function in (2) can be still reduced to

$$E_n(\vec{P}) \approx \sum_{x,y \in \Xi} \Re \left\{ \left[ I_{x,y,t}^t - (P_1x + P_2y + P_5 - x)I_{x,y,t}^x - \right. \right. \quad (3)$$

$$\left. \left. - (P_3x + P_4y + P_6 - y)I_{x,y,t}^y \right]^2, \sigma \right\} = \nabla I_{x,y,t} \quad (4)$$

In this equation,  $\nabla I_{x,y,t}$  represents the displacement at one location in an image to the spatial/temporal derivatives of intensity at the same location and  $\Re(\nabla I_{x,y,t}, \sigma)$  represents the usage of robust M-estimator function in the error function. And now the reduced form of the error function can be written as:

$$E_n(\vec{P}) \approx \sum_{x,y \in \Xi} \Re \left\{ \left[ r - \vec{q}^T \vec{P} \right]^2, \sigma_{cb} \right\} \quad (5)$$

where the vector  $\vec{q} = (xI^x \ yI^x \ xI^y \ yI^y \ I^x \ I^y)^T$  and the scalar  $r = (I^t + xI^x + yI^y)$ . This notation has been used for removing complexity of understanding the expressions. Thus imposing smoothness constraints on the adjacent points in the image plane replace the intensity gradient constancy assumption. So the error on the smoothness assumption  $E_s$  can be defined as:

$$E_s(\vec{P}) = \sum_{x,y \in \Xi} \left( \vartheta^T \left( \left( \frac{\partial \vec{P}}{\partial x} \right)^2 + \left( \frac{\partial \vec{P}}{\partial y} \right)^2 \right) \right) \quad (6)$$

$\vartheta^T \in Z^+$  contains six constant values for each parameters  $\vec{P}_1, \dots, \vec{P}_6$  that is used to control the smoothness constraint. Now the augmented robust error function is as follows:

$$E(\vec{P}) = \Re \left\{ E_n(\vec{P}) + E_s(\vec{P}), \sigma \right\} \quad (7)$$

This error function can now be minimized analytically by differentiating the error function with respect to its unknowns. The derivative of  $E_n(\vec{P})$  and  $E_s(\vec{P})$  are as follows

$$\frac{dE(\vec{P})}{d\vec{P}} = \sum_{x,y \in \Xi} \psi \left\{ \left[ \left[ r - \vec{q}^T \vec{P} \right]^2 + \vartheta^T \left[ \left( \frac{\partial \vec{P}}{\partial x} \right)^2 + \left( \frac{\partial \vec{P}}{\partial y} \right)^2 \right] \right], \sigma \right\} \quad (8)$$

Here  $\Re(x, \sigma) = \psi(x, \sigma)$  represents the robust influence function. Weight functions can be easily calculated from influence

function itself. Table-2 shows the relationship between weight and influence functions of the objective functions shown in Table-1.

Bringing the model into the gradient constraint (spatial/temporal derivatives) and considering all the pixels in the image at the same time, a linear influence system is solved by differentiating the error function with respect to its unknown affine parameters.

$$\frac{dE(\vec{P})}{d\vec{P}} = \frac{d \left( \left[ r - \vec{q}^T \vec{P} \right]^2 + \vartheta^T \left[ \left( \frac{\partial \vec{P}}{\partial x} \right)^2 + \left( \frac{\partial \vec{P}}{\partial y} \right)^2 \right] \right)}{d\vec{P}} = -2\vec{q}(r - \vec{q}^T \vec{P}) + 2\Phi(\int \vec{P} - \vec{P}) \quad (9)$$

$\int \vec{P}$  is the average of  $\vec{P}$  over a small neighborhood window in an image which enforces smoothing.  $\Phi$  is now the diagonal matrix with the diagonal elements of  $\vartheta^T$ . Make this equation to zero for solving  $\vec{P}$

$$\left[ \sum_{x,y \in \Xi} (\vec{q} * \vec{q}^T) + \Phi \right] \vec{P} - \left[ \sum_{x,y \in \Xi} (\vec{q} * r) + \Phi \int \vec{P} \right] = 0 \quad (10)$$

By solving this linear error system,  $\vec{P}$  has been calculated.

$$\vec{P} = \left[ \sum_{x,y \in \Xi} (\vec{q} * \vec{q}^T) + \Phi \right]^{-1} \left[ \sum_{x,y \in \Xi} (\vec{q} * r) + \Phi \int \vec{P} \right] \quad (11)$$

Now the iteration scheme starts by involving robust weight function  $W\left(\frac{F e_i}{\sigma}\right)$  for parameter estimation. An exact estimate of the error function during minimization can be regulated using Iterative reweighted least squares technique, where the weights are being modified on each iteration. Since the weights are generated by weight functions of various robust M-estimators, these weights are used to make the algorithm robust towards the outliers present in an image. The estimated parameters are fine-tuned on each iteration as follows.

$$\vec{P}_{j+1} = \left[ \sum_{x,y \in \Xi} \left( \vec{q} * W\left(\frac{F e_i}{\sigma}\right) * \vec{q}^T \right) + \Phi \right]^{-1} \left[ \sum_{x,y \in \Xi} \left( \vec{q} * W\left(\frac{F e_i}{\sigma}\right) * r \right) + \Phi \int \vec{P}_j \right] \quad (12)$$

where  $\vec{P}_j$  are the estimated parameters at iteration  $j$ .  $W$  is a diagonal matrix whose elements are weights of the chosen robust weight function and the residual  $F e_i = r - \vec{q}^T \vec{P}$ . At every level, the scale parameter  $\sigma$  for the weight function is calculated by using residuals of the error function at each minimization. The  $\sigma$  has been calculated using [23]

$$\sigma = 1.48 \text{ median} \left\{ \left| F e_i - \text{median}\{F e_i\} \right| \right\} \quad (13)$$

The iteration stops whenever the total squared error in each iteration does not show a substantial step-down with respect to the error in the previous iteration, or whenever a maximum number of iterations are achieved. In each iteration, the error function will be

$$E^2 = \sum_{i=1}^{I(N)} \frac{W_i F e_i^2}{\sum_{i=1}^{I(N)} W_i} \quad (14)$$

At the final step, the error function is minimized conceding desired affine parameters. Using the method described earlier (ANMO), affine parameters are estimated at each level of multiresolution pyramid. And now, these parameters are

used to warp the image in the next level of multiresolution pyramid. This process is repeated at all levels. For computing spatial/temporal derivatives, this method utilizes some set of derivative filters described in [24]. Since filtering and differentiation are linear operations, filtering the image directly with the derivative filters will be potentially improving the method. These filters are statistically significant and show the results in a beneficial manner. This work can be easily extended to 3D images in a straight forward manner. Here the number of parameters is extended to  $\vec{P} = (\vec{P}_1, \dots, \vec{P}_{12})^T$ , apart from radiometric parameters. We have worked only with 2D images and the results are shown for the same.

### III. RESULTS AND DISCUSSION

In this section, the proposed approach of affine parameter estimation is applied on real images to demonstrate its superior performance. Gaussian pyramid is constructed for source and target images using 5-tap low-pass filter. At each levels of resolution, local affine parameters are estimated for each neighborhood window of  $\Xi = 5 \times 5$  pixels of both source and target images and these parameters  $(P_1, \dots, P_6, P_7, P_8)$  are now used to find the smoothness assumption  $E_s$ .  $\vec{P}$  matrix is convolved over  $\Xi$  with  $3 \times 3$  smoothing kernel to find  $\int \vec{P}$ . Maximum of 20 iterations improves smoothness assumption and only few iterations on each level improve the parameter estimation to a greater extent. The initial estimate  $\vec{P}_{(0)}$  is calculated using least square technique. The proposed methodology (ANMO) is adopted on the multiresolution pyramid. The iterative fine-tune approach at every level of resolution will also make the updating of estimation parameters to almost reach the global minimum. And the results show that this acquainted non-convexity multiresolution based optimization approach gives an efficient robust affine parameter estimation. Matlab implementation of this method requires approximately 30 seconds for  $128 \times 128$  images on Pentium IV, 3 GHz, 512 MB RAM in Windows operating system. The affine model parameters are assigned as:

$$\begin{bmatrix} x' \\ y' \end{bmatrix} = \begin{bmatrix} a_{11} & a_{12} \\ a_{21} & a_{22} \end{bmatrix} \begin{bmatrix} x \\ y \end{bmatrix} + \begin{bmatrix} a_{13} \\ a_{23} \end{bmatrix} \quad (15)$$

where  $a$  denotes affine parameters. Table 3 shows the estimated affine model parameters for various brain atlas images which are taken from Harvard medical university website [25] and the mean error between actual and estimated affine parameters are also shown. Table 4 shows that the proposed ANMO based affine parameter estimation has small mean errors than any other other robust estimation approaches. Fig.3 shows the brain atlas images used for experimental studies.

### IV. CONCLUSION

A robust Affine parameter estimation using acquainted nonconvexity multiresolution based optimization (ANMO) has been proposed. The superiority of the proposed approach for robustly estimating the affine parameters has been demonstrated by experimental comparative study with other robust estimation techniques. A multiresolution strategy has been followed in order to reduce the complexity of the algorithm. With

TABLE II  
INFLUENCE FUNCTIONS AND ITS WEIGHTING FUNCTIONS

Function	Influence function $\psi(x, \sigma) = \Re'(x, \sigma)$	Weighting function $W(x, \sigma) = \frac{\Re'(x, \sigma)}{x}$
Charbonnier $E_{CH}$	$\frac{x}{\sqrt{1+(\frac{x}{\sigma})^2}}$	$\frac{1}{\sqrt{1+(\frac{x}{\sigma})^2}}$
Hebert-Leahy $E_{HL}$	$\frac{x}{1+(\frac{x}{\sigma})^2}$	$\frac{1}{1+(\frac{x}{\sigma})^2}$
Tukey's Biweight $E_T$	$x \left[1 - (\frac{x}{\sigma})^2\right]^2$	$\left[1 - (\frac{x}{\sigma})^2\right]^2$

TABLE III  
ESTIMATED AFFINE MODEL PARAMETERS USING ANMO APPROACH FOR SOURCE IMAGE OF VARIOUS BRAIN ATLAS IMAGES WITH VARIOUS NOISES

Brain Atlas Image	Noise	Parameters	$a_{11}$	$a_{12}$	$a_{21}$	$a_{22}$	$a_{13}$	$a_{23}$
Pick's Disease	Gaussian	Actual	0.9950	0.0995	-0.0995	0.9950	0.0000	0.0000
		Estimated	0.9935	-0.0039	0.0009	1.0034	0.0798	-0.0300
	Salt&Pepper	Actual	0.9950	0.0995	-0.0995	0.9950	0.0000	0.0000
		Estimated	1.0011	-0.0002	0.0007	0.9994	0.0649	-0.0432
Huntington Chorea	Gaussian	Actual	0.9950	0.0995	-0.0995	0.9950	0.0000	0.0000
		Estimated	0.9980	0.0024	-0.0017	0.9988	0.0455	-0.0556
	Salt&Pepper	Actual	0.9950	0.0995	-0.0995	0.9950	0.0000	0.0000
		Estimated	0.9968	0.0010	-0.0000	1.0013	0.0408	-0.0419
Cerebrovascular Fatal stroke	Gaussian	Actual	0.9950	0.0995	-0.0995	0.9950	0.0000	0.0000
		Estimated	0.9967	-0.0018	0.0023	0.9972	0.0431	-0.0139
	Salt&Pepper	Actual	0.9950	0.0995	-0.0995	0.9950	0.0000	0.0000
		Estimated	1.0008	0.0020	0.0003	0.9977	0.0567	0.0504
		Mean Error	0.033	0.0966	-0.0985	0.0046	0.0551	-0.0392

TABLE IV  
MEAN ERRORS OF ESTIMATED AFFINE MODEL PARAMETERS FOR VARIOUS ROBUST ESTIMATION METHODS.

Methods	Mean Errors					
	$a_{11}$	$a_{12}$	$a_{21}$	$a_{22}$	$a_{13}$	$a_{23}$
Tukey's Biweight	0.0326	0.1822	-0.1278	0.0958	0.1294	-0.1104
Hebert Leahy	0.0126	0.1108	-0.1056	0.0258	0.0987	-0.0754
ANMO	0.0033	0.0966	-0.0985	0.0046	0.0551	-0.0392



Fig. 3. (a) Pick's Disease (b) Huntington Chorea (c) Cerebrovascular Fatal Stroke; Courtesy to:[25]

the objective to estimate the exact affine parameters, this paper suggests the use of various robust functions that gradually acquaints nonconvexity as the multiresolution pyramid reaches its finer level of resolution. This new proposal considerably improves the power of parameter estimation in all kind of images and hence one can say that the proposed approach achieved the worthy level of applicability.

#### REFERENCES

- [1] S. Geman and D. Geman, Stochastic relaxation, Gibbs Distributions and the Bayesian restoration of Images, *IEEE Trans. on Pattern Analysis and Machine Intelligence*, 6, 721-741, 1984.
- [2] F. C. Jeng and J. W. Woods, Image estimation by stochastic relaxation in the compound Gaussian case, In *Proceedings IEEE Conf. on Acoust., Speech, and Signal Proc.*, 1988.
- [3] S. Kirkpatrick and C. D. Gelatt and M. P. Vecchi, Optimization by Simulated Annealing, *Science*, 220(4598), 671-680, 1983.
- [4] K. Matsui, M. Sase and Y. Kosugi, Medical Image Mapping Using Collaborative Genetic Algorithm, In *Proceedings of Sixteenth Annual International Conference of the IEEE Engineering in Medicine and Biology Society*, Baltimore, Maryland, U.S.A., 1(2), 612-613, 1994.
- [5] B.C.S. Tom, S.N. Efstratiadis and A.K. Katsaggelos, Motion Estimation of Skeletonized Angiographic Images Using Elastic Registration, *IEEE Transactions on Medical Imaging*, 13(3), 450-460, 1994.
- [6] V.R. Mandava, J.M. Fitzpatrick and D.R. Pickens, Adaptive Search Space Scaling in Digital Image Registration, *IEEE Transactions on Medical Imaging*, 8(3), 251-262, 1989.
- [7] S. Farsiu, D. Robinson, M. Elad, and P. Milanfar, Fast and Robust Multi-frame Super-resolution, *IEEE Transactions on Image Processing*, 13(10), 1327-1344, 2004.
- [8] Ming Ye, Linda G. Shapiro, Robert M. Haralick, Estimating Piecewise-Smooth Optical Flow with Global Matching and Graduated Optimization, *IEEE Transactions on Pattern Analysis and Machine Intelligence*, 25(12), 1625-1630, 2003.
- [9] C. Koch, J. L. Marroquin, and A. L. Yuille, Analog neuronal networks in early vision, In *Proceedings of the National Academy of Sciences*, pp. 4263-4267, 1986.
- [10] D. Geiger and F. Girosi, Parallel and deterministic algorithms for MRFs: surface reconstruction and integration, Technical Report A. I. Memo, No. 1114, Artificial Intelligence Lab, M. I. T, 1989.
- [11] D. Terzopoulos, The Computation of Visible-Surface Representations, *IEEE Transactions on Pattern Analysis and Machine Intelligence*, 10, 417-437, 1988.
- [12] M. Lefebvre and L. Cohen, A multiresolution algorithm for signal and image registration, in *Proc. IEEE Int. Conf. on Image Processing*, 3, 252-255, 1997.
- [13] A. Blake, A. Zisserman, Visual Reconstruction, *MIT Press*, Cambridge, MA, 1987.
- [14] P. J. Green, Bayesian reconstructions from emission tomography data

- using a modified EM algorithm, *IEEE Transactions on Medical Imaging*, 9, 84–93, 1990.
- [15] R. R. Schultz and R. L. Stevenson, Stochastic modeling and estimation of multispectral image data, *IEEE Transactions on Image Processing*, 4, 1109–1119, 1995.
- [16] C. Bouman and K. Sauer, A generalized Gaussian image model for edge-preserving MAP estimation, *IEEE Transactions on Image Processing*, 2, 296–310, 1993.
- [17] K. Lange, Convergence of EM image reconstruction algorithms with Gibbs smoothing, *IEEE Transactions on Medical Imaging*, 9, 439–446, 1990.
- [18] Pierre Charbonnier, Laure Blanc-Fraud, Gilles Aubert, Michel Barlaud, Deterministic edge-preserving regularization in computed imaging, *IEEE Transactions on Image Processing*, 6(2), 298–311, 1997.
- [19] R. Dahyot, P. Charbonnier, and F. Heitz, Robust visual recognition of colour images, In proceedings of *CVPR*, 1, 685–690, 2000.
- [20] T. Hebert and R. Leahy, A generalized EM algorithm for 3-D Bayesian reconstruction from Poisson data using Gibbs priors, *IEEE Transactions on Medical Imaging*, 8, 194–202, 1990.
- [21] Roger M. Dufour, Eric L. Miller, Nikolas P. Galatsanos, Template matching based object recognition with unknown geometric parameters. *IEEE Transactions on Image Processing*, 11(12), 1385–1396, 2002.
- [22] Michael J. Black, P. Anandan, The Robust Estimation of Multiple Motions: Parametric and Piecewise-Smooth Flow Fields, *Computer Vision and Image Understanding*, 63(1), 75–104, 1996.
- [23] P. W. Holland and R. E. Welsch, Robust regression using iteratively reweighted least-squares, *Communications in Statistics: Theory and Methods*, A6, 813–827, 1977.
- [24] H. Farid and E.P. Simoncelli. Optimally rotation-equivariant directional derivative kernels. In *Proceedings of International Conference on Computer Analysis of Images and Patterns*, pp. 207–214, Berlin, Germany, 1997.
- [25] Keith A. Johnson, J. Alex Becker, The whole brain Atlas, <http://www.med.harvard.edu/AANLIB/>



**J. Dinesh Peter** is a Assistant Professor in the department of Computer Science and Engineering at KMCT College of Engineering - Calicut - Kerala - India. His research interests are image processing and robust statistics.